Second Harmonic Light Generation in the Interaction of Laser Beams with Undercritical Plasmas

D. Batani, A. Giulietti, V. Biancalana, F. Bianconi, M. Borghesi, P. Chessa,
D. Giulietti, L. Gizzi, I. Deha, and E. Schifano

Abstract
The process of second harmonic generation (SHG) in undercritical plasmas is studied. It is shown that filamentation and self-focusing of the laser beam in the plasma can break the plasma density symmetry and lead to SHG by free electrons. In turn, second harmonic emission may be used to investigate the plasma parameters and to diagnose the process of laser beam filamentation itself.

Key words: harmonic generation, self-focusing, plasma interactions, plasma diagnostics, nonlinear optics

1. INTRODUCTION

In nonlinear optical media the polarization of the system P must be written (using the scalar approximation) as a function of the applied electric field E as

$$P = \chi_1 E + \chi_2 E^2 + \chi_3 E^3 + \dots . \quad (1)$$

When the system is perturbed with a monochromatic electromagnetic (EM) wave (e.g., laser radiation) with frequency ω, we have polarization waves oscillating at frequencies ω, 2ω, and so on. This in turn produces emissions of harmonics.

It is well known that in isotropic media (in particular gases) the quadratic term, owing to symmetry, must vanish: $\chi_2 = 0$. As a consequence, second harmonic generation (SHG) is a forbidden process in homogeneous plasmas and gases.

Let us instead consider strongly inhomogeneous plasmas and, in particular, regions whose density is close to the plasma critical density, that is, the maximum (electron) density at which EM radiation can penetrate in the plasma, given by

$$n_e = n_c = 1.1 \times 10^{21}/\lambda^2, \quad (2)$$

with n_e in cubic centimeters and wavelength λ in micrometers. In the layers where $n_e \simeq n_c$ the laser frequency equals the plasma frequency

$$\omega_L \simeq \omega_p = (4\pi n_e e^2/m_e)^{1/2}; \quad (3)$$

hence, with laser-produced plasmas and high-intensity laser beams we can have the excitation of plasma waves or "plasmons." This is the "resonant absorption" process and is possible thanks to the steep density (and above all refraction index) gradient near the critical surface. The plasmons may then couple with the incoming laser wave (p + 1) or with another plasmon (p + p) to produce 2ω light. This is resonant nonlinear optical behavior as with the interaction of atomic systems with laser light of frequency close to one atomic transition. SHG from critical layers has been proven experimentally and has been widely used as a plasma diagnostic in inertial confinement fusion experiments.

However, in a few experiments with high laser intensities, SHG has been detected even from undercritical plasmas where the hydrodynamic density gradients (those connected with the laser beam spot size and produced by plasma expansions) are indeed very weak. In other words, at high intensities, even an undercritical plasma ($n_e < n_c$) will behave as a (nonresonant) nonlinear medium. In this paper we show that in this case SHG must mostly be related with self-focusing and filamentation instability (FI).

Since the FI is due to the χ_3 term and the SHG due to the χ_2 term, there is no direct link between FI and SHG. The main point is that the laser itself, via the FI, produces the density gradients that may then produce SHG. Hence SHG can be used as a useful diagnostic for filamentation. This is very important for the field of inertial nuclear fusion. Indeed, filamentation in the (undercritical) plasma corona of the fusion pellet may alter energy distribution in the beam and energy deposition on the target, contributing to a degradation of the compression uniformity and bringing a premature end to the implosion. Moreover, filamentation can cause a local strong increase in laser intensity and hence open the way to laser plasma instabilities with a much higher intensity threshold, which are very detrimental to laser plasma coupling.

2. SHG IN UNDERDENSE PLASMAS: THEORETICAL MODEL

A realistic model that illustrates SHG in plasma is the free electron gas model. This model was originally introduced to explain optical nonlinearities due to plasma in metals and the observation of SHG from metal surfaces.[1] This was evidenced in the early 1960s, shortly after the discovery of lasers, and it was shown that the plasma contribution is usually much larger than the nonlinear contribution arising from interband transitions of the valence electrons.

In this model the equation of motion and the continuity equation are used to describe the spatial and time variations of electron density and velocity. In the last equation we assume for simplicity that the pressure gradient term is zero ($\nabla p = 0$) and that there is a fixed positive charge background in the plasma which assures charge neutrality in the absence of external perturbations. The expression of the 2ω currents turns out to be[2]

$$\begin{aligned}\mathbf{J}_{2\omega} &= e(n_e\mathbf{v}^{(2)} + n_e^{(1)}\mathbf{v}^{(1)}) \\ &= \frac{in_e e^2}{2m_e^2\omega^2}\left[\frac{1}{i4\pi}(\nabla\cdot\mathbf{E})\mathbf{E} + \frac{e}{m_e^2\omega}(\mathbf{E}\cdot\nabla)\mathbf{E} + \frac{ie}{m_e c}(\mathbf{E}\times\mathbf{B})\right] \\ &= \frac{ie^3}{\omega^3 m_e}\left[\left(\nabla n_e\cdot\frac{\mathbf{E}_\omega}{\epsilon_\omega}\right)\mathbf{E}_\omega + \frac{n_e}{4}\nabla(\mathbf{E}_\omega\cdot\mathbf{E}_\omega)\right],\end{aligned} \tag{4}$$

where $\mathbf{v}^{(1)}$, $\mathbf{v}^{(2)}$, and $n_e^{(1)}$ are the first- and second-order corrections to electron velocity and density. The last term is due to Lorentz force; indeed, since in a plasma $v \ll c$, the Lorentz force is much weaker than the coulomb force and can be treated as a perturbation in the successive approximation of the solution. The other is related to spatial variation of the electric field and electron density.

Finally, ϵ is the plasma dielectric constant

$$\epsilon = 1 - \omega_p^2/\omega^2, \tag{5}$$

which for an undercritical plasma is close to 1 (at a fixed density this is even more so for the 2ω radiation).

We note that the $\mathbf{J}_{2\omega}$ current cannot radiate if the plasma is homogeneous. Indeed, if n_e is independent of position, the first term is identically zero. Besides, the gradient term in Eq. (4) gives a purely irrotational polarization (with vanishing curl) which cannot radiate in bulk media (although at boundaries it can give a radiating dipole layer).

It is also easy to see that this current is different from zero only if there are density gradients in the direction perpendicular to that of the laser beam propagation (indeed, since $E = E_\perp$, only the terms of the kind $E_\perp^2\nabla_\perp n_e$ are nonvanishing). Hence SHG is strictly connected to the presence of steep perpendicular gradients such as those created by filaments in the plasma.

The SH magnetic field is then related to the source currents by[3,4]

$$\mathbf{B}_{2\omega} = \frac{i\mathbf{k}_{2\omega}}{cR}\times\int\mathbf{J}_{2\omega}e^{-i\mathbf{k}_{2\omega}\mathbf{r}}dV; \tag{6}$$

hence

$$\begin{aligned}\mathbf{B}_{2\omega} &= \frac{i\mathbf{k}_{2\omega}}{cR} \\ &\times\int dz\exp(-ik_{2\omega}z\cos\psi)\int d^2\mathbf{r}_\perp\exp(-ik_{2\omega}\hat{R}\cdot\mathbf{r}_\perp)\mathbf{J}_{2\omega},\end{aligned} \tag{7}$$

where R is the distance from the filament to the observer, $\hat{R}$ the associate versor, and ψ is the angle between R and the filament axis z. The transverse variation of electric field and electron density occurs over scale lengths of the order of the filament diameter, which may be as small as a few optical wavelengths. In the axial direction, however, their variation occurs over a much larger distance $l_F \gg \lambda$ characteristic of the effective filament length.

Since the 2ω currents contain an $\exp(2ik_\omega z)$ term, if we suppose that $k_{2\omega} \simeq 2k_\omega$, it is easy to see that the z integration over the factor $\exp[-ik_{2\omega}(1-\cos\psi)z]$ would average nearly to zero except around the forward direction $\psi \simeq 0$. The angular width of this forward radiation pattern is approximately $\Delta\psi \simeq (2\lambda/l_F)^{1/2}$. In reality, if we can neglect the ∇n_e term, $\mathbf{J}_{2\omega}$ is proportional to $\mathbf{E}\times\mathbf{B}$, and this is only along the direction of beam propagation. Hence, since an oscillating current cannot radiate longitudinally, we expect no coherent SHG exactly along the axis of propagation.

Even in the more general case, since the pump intensity and the electron density are both assumed to be cylindrically symmetric and have transverse dimension $\simeq L_\perp$, where $L_\perp$ is the perpendicular scale length, to first approximation the gradient operator $\nabla_\perp$ brings down a factor proportional to $\mathbf{r}_\perp/L_\perp^2$ whether it is applied to n_e or to E_ω^2. Because of this factor, the 2ω radiation will be emitted off-axis and in a narrow cone around the beam axis.

Let us now suppose that we have another fundamental wave, $\mathbf{E}_B$, within the filament propagating back toward the laser. This wave in undercritical plasmas can only arise from stimulated Brillouin backscattering (SBS) generated in the bulk of the plasma or within the filament itself. In this case the expression of the source currents will contain all the terms such as

$$\begin{aligned}\mathbf{J}_{2\omega} &= \frac{ie^3}{\omega^3 m_e^2}\nabla n_e\cdot\left[\mathbf{E}_\omega\mathbf{E}_\omega\exp(ik_{2\omega}z)\right. \\ &\left. + \mathbf{E}_B\mathbf{E}_B\exp(-ik_{2\omega}z) + \mathbf{E}_\omega\mathbf{E}_B + \mathbf{E}_B\mathbf{E}_\omega\right].\end{aligned} \tag{8}$$

Now the second term would produce a 2ω wave in the backward direction ($\psi \simeq \pi$), but the last two terms produce a contribution normal to the filament. Indeed, the z integration will maximize for $\psi \simeq \pi/2$ with an effective angular width

$\Delta\psi \simeq \lambda/l_p$. In this case it is easy to show that SHG is strictly connected to the presence of perpendicular gradients.

From Eq. (8) we see that the "harmonic" frequency is really a frequency sum of the forward and Brillouin backscattered waves. In reality, $\omega_B < \omega_L$, the backward wave being slightly Stokes-shifted by the ion-acoustic wave, and this shift is also present in the harmonic radiated normally, whose exact frequency is $\omega_L + \omega_B = 2\omega_L - \omega_i$, where ω_i is the ion-acoustic frequency. In addition, if the plasma is moving, to obtain the real shift we must also take into account the Doppler effect, which produces an additional shift, $\Delta\omega_D$. Since the dispersion relation for ion-acoustic waves is approximately

$$\omega_i = (ZT_e/M_i k_i)^{1/2} = c_s k_i, \tag{9}$$

where T_e, M_i, Z, k_i, and c_s are, respectively, the electron temperature, the ion mass, the ion charge, the wave vector of the ion acoustic wave and its velocity, then it is possible to measure the plasma temperature by measuring the 2ω shift. SBS is indeed often used as a plasma diagnostic in laser plasma experiments. We have now shown that even the 2ω radiation emitted at 90° can be used as a diagnostic for both filamentation and the process of SBS, carrying information on plasma temperature and flow. This is in principle very interesting; indeed, in the "pure" SBS diagnostics, radiation must be collected in the backward direction and, being very close in frequency to the fundamental one, must be accurately spectrally separated from the scattered and reflected fundamental radiation. It can then be a great advantage to measure radiation emitted at a different angle and in a different spectral window. Moreover, the ratio between 2ω emitted forward and at 90° should give, almost directly, the "efficiency" of SBS.

3. SHG: EMISSION FROM PLASMAS PRODUCED FROM GASES

SH emission in the forward direction from ionized gases was initially reported in Refs. 5 and 6 and theoretically analyzed by Bethune in Ref. 7. Only in the second experiment could SHG be attributed to the presence of free electrons in the plasma. However, even in this case SHG was not due to the oscillating 2ω currents given by (4), but rather was due to the development of a radial electric field $\mathbf{E}_S$ as a consequence of ponderomotive forces (radiation pressure) and finite kinetic energy of the free electrons created by photoionization of gas molecules in the laser beam. These expelled electrons from the laser beam and hence created a charge separation and a dc electric field which coupled, via the χ_3 term, with EM fields oscillating at ω to produce a 2ω polarization charge.

The contribution of 2ω free electron currents was negligible due to the low electron density produced in those experiments ($n_e \simeq 10^{16}$ cm^{-3}). However, it was predicted that this term should become dominant at higher electron densities. These conditions were reached in an experiment performed at IFAM[8,9] at $n_e \simeq 10^{19}$ cm^{-3}, which clearly showed SHG due to the $\mathbf{J}_{2\omega}$ currents, that is, due to a χ_2 term. The experimental setup used at IFAM is shown in Fig. 1. In the experiment a laser beam with

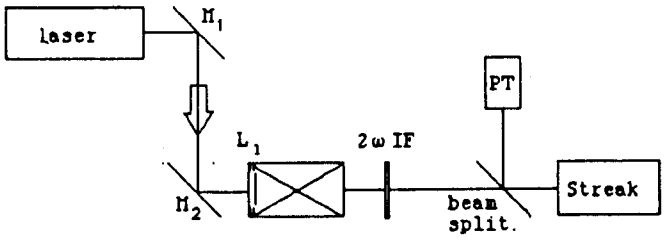

Figure 1. Experimental setup used in the SHG experiment at IFAM. M_1 and M_2 are mirrors; L_1 is the focusing f/20 lens; IF is the interferential filter; and PT is the photomultiplier.

pulse length $t_L = 20$ ns and energy per pulse $E_L \leq 20$ J was focused at intensities $I_L \simeq 10^{13}$ W/cm^2 into helium gas to produce a fully ionized plasma with electron temperature $T_e \simeq 50$ eV. The 2ω radiation was detected in the forward direction (but not in other directions) with a phototube. In addition, 2ω sources, localized in the beam waist, were imaged on the slit of a streak camera coupled to an interference filter which allowed one-dimensional time-resolved images to be obtained.

In Fig. 2 we show the experimental results for 2ω conversion efficiency (which is defined as the ratio of ω and 2ω powers, i.e., $\gamma = P_{2\omega}/P_\omega$) as a function of helium gas pressure, while in Fig. 3 we show γ as a function of laser power.

The fairly complicated trend of experimental data can be explained from the usual expression of $P_{2\omega}$ in the approximation of plane EM wave and cylindrical symmetry[10] that is reasonable for our experiment,

$$P_{2\omega} = \frac{32\pi^2\omega^2 P_\omega^2}{a^2c^3}\chi_{2\omega}^2 L^2 F(\Delta k). \tag{10}$$

Here, L is the plasma length and a the beam radius. The nonlinear susceptibility $\chi_{2\omega}$, which we find in the expression of the nonlinear polarization $P_{NL}(2\omega) = \chi_{2\omega}E^2(2\omega)$, must be calculated from expression (4) of the 2ω currents. We must use the wave equation for the 2ω fields,

$$[\nabla \times (\nabla \times) + (\epsilon/c^2)(\partial^2/\partial t^2)]E_{2\omega} = (4\pi/c^2)(\partial J_{2\omega}/\partial t) = (4\pi/c^2)(\partial^2/\partial t^2)P_{NL}(2\omega), \tag{11}$$

where the source term can be written as a function of the nonlinear polarization or, equivalently, of the source currents. The result is

$$\chi_{2\omega} = \frac{n_e}{L_\perp}\frac{e^3}{2\omega^4 m_e^2}. \tag{12}$$

This coincides with the result first obtained by Bethune[7] except for the $2/L_\perp$ factor, which is due to the different defini-

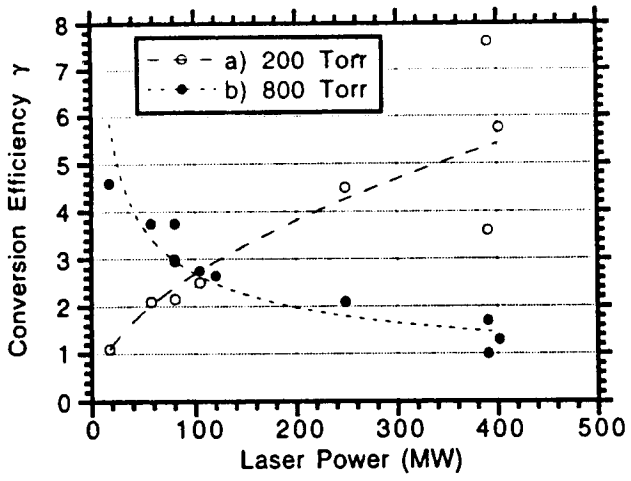

Figure 2. γ versus laser power (MW) for helium densities of 200 Torr (curve a) and 800 Torr (curve b) corresponding to $n_e = 7 \times 10^{18}$ and 3×10^{19}, respectively.

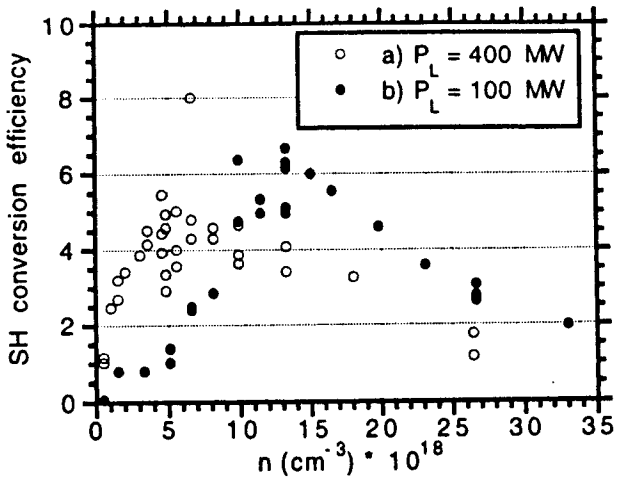

Figure 3. γ versus helium density for laser powers equals 400 MW (curve a) and 100 MW (curve b).

tion of $\chi_{2\omega}$ (indeed, he uses $P_{NL} = 2\chi_{2\omega}\nabla_\perp E^2$). In Eq. (10) the function $F(\Delta k)$ is a phase-matching function whose maximum value is 1. For example, it is well known that in the case of uniaxial crystals it is

$$F(\Delta k) = \frac{\sin^2(\Delta kL)}{(\Delta kL)^2}. \tag{13}$$

In uniaxial crystals it always possible to choose the direction of the laser beam with respect to the crystal optical axis in such a way that the indexes of refraction for the ω and 2ω radiation are the same (phase-matching direction). We then have $\Delta k = 0$ and $F = 1$, and $P_{2\omega}$ increases as L^2 (until there is no depletion of the pump beam). In all other directions $P_{2\omega}$ is an oscillating function of medium length.

In our case the optical axis is forced to coincide with the laser axis, the laser beam being the source of anisotropy, and hence the phase matching is not possible. To calculate the order of magnitude of 2ω emission, we can then consider a plasma length equal to the coherence length l_c, which is defined as

$$l_c = \pi/(2\Delta k) \tag{14}$$

(only emission from a plasma layer of length l_c will add in a coherent way). From the EM dispersion relation we can calculate

$$\Delta k = k_\omega n_e/n_c = \omega n_e/cn_c. \tag{15}$$

Using this result we see that conversion efficiency γ is not explicitly dependent on the background electron density n_e.

To fully explain our experimental data, we must also consider the absorption length l_ω for laser light in the plasma. For $l_\omega \ll L$, in the low absorption regime (which is verified for atomic densities $\leq 10^{19}$ cm^{-3}), we note from Fig. 3 an increase of γ with density. Since γ is independent of n_e, this is really due to the fact that the growth length for FI decreases at higher densities, and hence the effective beam radius $a \simeq L_\perp$ decreases. The above explanation is also consistent with the slope of the curve (a) of Fig. 2. Indeed, for a given density the conversion efficiency is expected to rise with the laser power.

For $l_\omega \gg L$, in the high absorption regime, the plasma was found to grow mainly towards the focusing lens. This means that the laser is absorbed in a layer whose thickness decreases with density, and that the interaction intensity keeps a value comparable with the gas breakdown threshold E_{bt}. SHG may only take place in that layer, and since the E_{bt} value decreases with increasing gas density, then γ apparently decreases, as shown in Fig. 3 (in reality, a progressively smaller fraction of laser electric field is effectively involved in the SHG process). For a fixed (high) density, γ consistently decreases like E_{bt}^2/P_ω as shown in the curve (b) of Fig. 2.

We also note the maximum of conversion efficiency shifts to lower densities going from 100 MW - 400 MW laser power. This is due to the fact that optimal conditions for FI instability growth are reached at smaller plasma densities for higher laser power. The 2ω angular distribution was also measured. The 2ω light was emitted in a cone around the forward direction with no intensity exactly on axis and a maximum at 2° from it, in agreement with the theory. The 2° emission angle was also consistent with emission from filaments of size 10 μm or less.[8]

Finally, Fig. 4 shows a time-resolved forward image. Here it is possible to see 2ω emitting filaments as submicron structures ($d \leq 10\mu$m), with a lifetime of a few nanoseconds, localized within the laser beam.

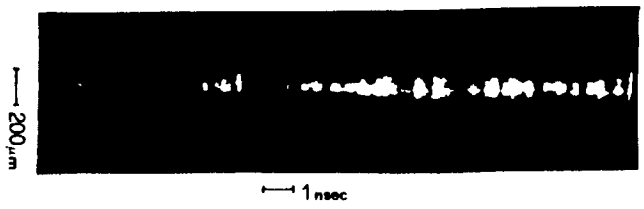

Figure 4. Evidence of filaments in the plasma. The beam diameter is vertical (average 100 μm); time is horizontal and increases towards the right. Modulations on the 100 ps time scale closely follow those of the laser pulse.

No SHG at large angles from ionized gases has been reported in the literature. Our experimental attempt to detect SHG at 90° from plasmas produced from gases produced no results in the limit of detection of our experimental apparatus.

4. SHG: FORWARD EMISSION FROM EXPLODING FOIL PLASMAS

Higher electron densities n_e can be obtained from exploding foil plasmas. In a series of experiments we replaced the gas-filled cell by an in-vacuum interaction chamber containing a thin foil plastic target (FORMVAR with typical thickness $\simeq 1$ μm) in the lens focus. The laser pulse length was also changed to t_L = 3 ns. The foil was "thin" in the sense that it completely burned through at the beginning of the laser pulse, leaving an undercritical plasma to interact with the laser beam.

Again,[11] we recorded conversion efficiency γ as a function of laser power P_ω. Results are shown in Fig. 5 where curve (a) shows γ when the target was "in focus" and curve (b) the same with the target "out of focus," that is, $\simeq 1$ mm from the position of the laser focal spot. We see that while (b) shows a quasilinear behavior, curve (a) is much steeper. Indeed, in this case $P_{2\omega}$ scales approximately as P_ω^3.

Again, in analogy with what was observed in gases with Fig. 2, the deviation from a quadratic scaling of $P_{2\omega}$ versus P_ω (i.e., linear scaling of γ with $P\omega$) shows that other nonlinear phenomena enter into the SHG process which can "boost" SH conversion efficiency. Again, the causes of such deviation are the ponderomotive and thermal effects which can drive laser beam filamentation in the plasma.

Direct evidence of filamentary structures in the plasma was provided by 2ω forward imagery. In this case the streak camera was replaced by a fast-framing camera with a 120 ps gate time which allowed two-dimensional time-resolved images to be collected. One such image is shown in Fig. 6, where one can clearly see how SH emission comes from small circular regions, approximately 5 μm in diameter, which are well localized in the center of the laser focal spot. The transverse dimension of 2ω sources, measured on time-resolved images collected at 90° with a streak camera, clearly shows that at the time of 2ω emission the plasma is undercritical.

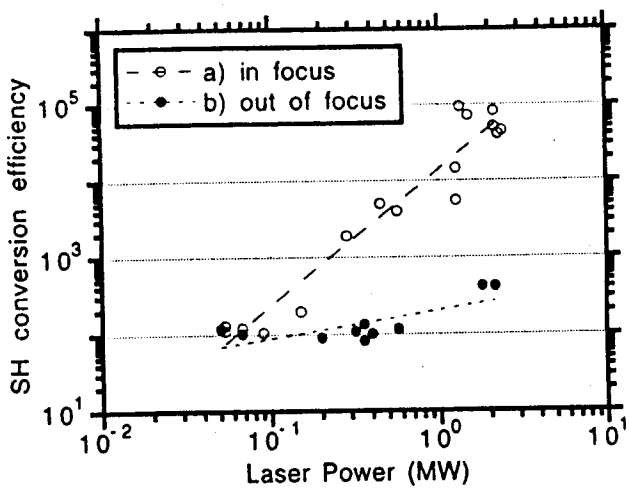

Figure 5. γ versus laser power recorded with thin foil targets in the laser focus (curve a) and out of focus (curve b).

5. SHG: SIDE EMISSION FROM THIN FILMS

The higher density of the underdense plasmas produced from thin foils (typically $n_e \simeq 10^{20}$ cm^{-3}) makes it much more likely for SBS to occur, and, hence, Eq. (8) should be valid. This explains why we can observe 90° 2ω emission with plasmas produced from thin foils while there was no such an emission from gases. However, a calculation of the SBS threshold in our experimental conditions[12] gives an intensity threshold still bigger than the nominal intensities used in the experiment. Hence in our experimental conditions, not only is filamentation necessary to produce the perpendicular gradients necessary for SHG, but the presence of SBS itself must be related to filamentation which can easily produce an increase of up to 100 times in the local laser intensity.

The first experimental evidence of SHG at 90° with undercritical plasmas was given in the Stamper *et al.* experiment[13] where 2ω emitting filamentary structures were photographed in the $n_e \ll n_c$ plasma region. In that case two-dimensional images at 90° were collected with a normal (time-integrating) camera, coupled to an interferential filter, which was imaging the plasma corona of a thick foil plastic target. The images showed that filament-shaped regions were the sources of 2ω emission, but the apparatus used in the experiment did not allow a measure of the 2ω spectral shift (incidentally, the ω wave propagating backward in the experiment was more likely produced by reflection from the critical surface rather than by SBS).

In the experiment at IFAM,[14] SH emitted at 90° was sent to a visible spectrometer whose output slit was imaged with a streak camera to obtain time resolved 2ω spectra, one of which is shown in Fig. 7.

The spike behavior of the spectrum is connected to laser intensity modulations already present in the beam, as in Fig. 4, which are enhanced by the nonlinear SHG process. We see that

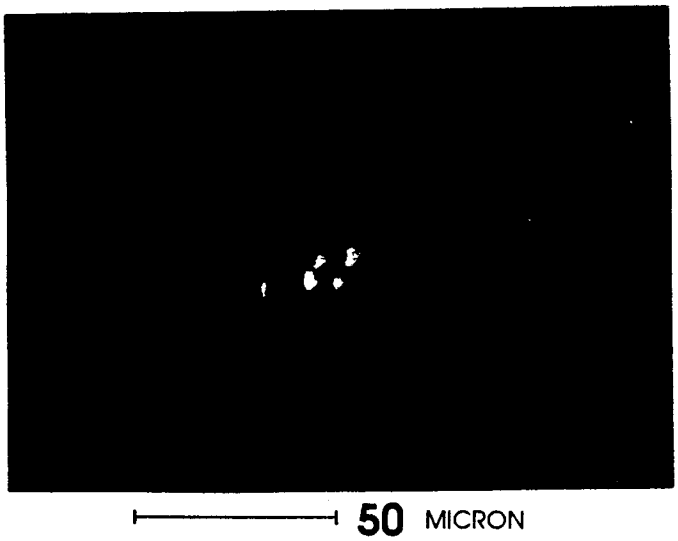

Figure 6. 2ω source images recorded with a gated camera in the forward direction. Exposure time corresponded to 120 ps around the laser intensity peak.

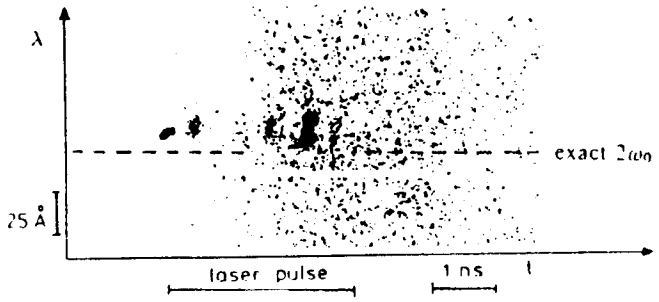

Figure 7. SH time-resolved spectrum obtained by irradiating a formvar foil with diameter $d = 1.58$ μm by laser light with $\lambda = 1.06$ μm, $t_L = 3$ ns, and $I = 1.4 \times 10^{13}$ W/cm^2.

the spectrum is redshifted with respect to the "real" 2ω and that the redshift is increasing with time.

If we assume that this shift is given by Eq. (9), and note that the shift at 2ω is half the value at ω, we see that the measured initial shift, $\Delta\lambda \simeq 4$ Å, corresponds to a temperature $T_e \simeq 600$ eV. This is in agreement with the prediction of self-similar expansion models,[12] once two-dimensional corrections are taken into account. Such models also predict that such a temperature should be approximately constant around the laser pulse peak. The time variation of the 2ω shift is then due to the Doppler effect resulting both from whole plasma motion in the direction of the laser beam with velocity v_p and from plasma expansion around the center of mass. We can measure a maximum plasma velocity $v_p \simeq 6 \times 10^7$ cm/s about 2 ns after the beginning of the 2ω emission. The doublet structure in the spectrum means then that two plasma regions, moving in opposite directions, are more active in SBS, and we can infer that these are the sonic layers (since $v \simeq c_s$ as can be seen from Fig. 7).

The assumptions regarding the doublet structure in the 2ω spectrum were partially confirmed by an experiment[15] conducted at LULI, Ecole Polytechnique, where the 2ω light emitted from the front and back sides of the expanding plasma were separately collected and spectrally time resolved. The experiment clearly showed differences in the two spectra even if the motion of the target plasma did not allow a definite separation of the two regions.

The results of these experiments prove that not only SHG is related to laser beam filamentation in the plasma, but SH itself can be used as a plasma diagnostic both to measure plasma parameters (via SBS) and to detect filamentation itself.

A recent, interesting experiment by Young *et al.*[16] has partially confirmed these results, but has also shown that not all the filament volume contributes in the same manner to 2ω emission. In the experiment, thin foil plastic targets were irradiated by laser radiation to preform an underdense plasma which was subsequently irradiated with another line-focused laser beam. The interaction of this last beam with the plasma was studied by means of time-resolved interferograms to measure produced density perturbations, connected to laser beam filamentation, and these results were compared to simultaneous gated images of SH images.

SHG and density perturbations were shown to be spatially correlated, that is, the peak of 2ω emission occurred in the density perturbations, probably at the position of the peak incident intensity. Anyway, there were differences in the position of this peak inside the filament probably due to the fine dynamics of the self-focusing process and refraction of 2ω rays propagating through the filament. In general, SHG was not taking place homogeneously in the filament, but 2ω sources were preferentially located closer to the higher density regions of the plasma.

The doublet structures evidenced in the Giulietti *et al.* experiment,[14] which was related to the spatial position of SBS sources, also shows that the spatial relation between filaments and 2ω sources is rather complicated and cannot be simplified as a uniform 2ω emission from the whole filament. Young *et al.* also suggested that the results of Stamper *et al.* experiment, that is, a long longitudinal extension of 2ω sources observed in time integrated images, could be interpreted as a result of filament focus motion during plasma and laser pulse evolution.

In our opinion, these results are very interesting but are not yet conclusive; clearly, more research is needed to clarify this point. In particular, the experiments by Young *et al.*[16] and Giulietti *et al.*[14] are not easily comparable to that by Stamper *et al.*,[13] since in the latter case the plasma was produced from a thick foil solid target, and a critical layer was always present during laser plasma interaction and could reflect incident radiation. While, in general, with thin films the experimental situation is much more controllable than with thick targets, the relative amount of SBS in the two cases may be completely different (not to mention light reflected from the critical

surface), and was not measured in those experiments. In particular, experiments with thin foils could produce a smaller SBS, and the backpropagating wave could even be depleted by plasma absorption or by the SHG process itself. This could not be the case in experiments with thicker targets.

6. CONCLUSIONS

The results of the experiments discussed here show that laser beam filamentation in undercritical plasmas can break the plasma density isotropy and lead to SHG produced by free electrons. In turn, SHG can be used as a useful diagnostic for filamentation. This is very important for inertial confinement fusion. Indeed, filamentation in the (undercritical) plasma corona of the fusion pellet may alter energy distribution in the beam and energy deposition on the target, contributing to a degradation of the compression uniformity and bringing an early end to the implosion. Moreover, filamentation can cause a local strong increase in laser intensity and hence open the way to laser plasma instabilities, with a much higher intensity threshold, which are very detrimental to laser plasma coupling. Still, some aspects of SHG need to be clarified, in particular, the exact position of 2ω sources and their spatial relation with SBS.

Acknowledgment

We thank Professor E. Sindoni, University of Milano, for his kind interest. We also thank Professor O. Willi, Imperial College, London, and Professor C. Labaune, LULI, École Polytechnique, Palaiseau, for their useful suggestions.

APPENDIX: SELF-FOCUSING AND FILAMENTATION OF LASER BEAMS IN PLASMAS

Let us consider a laser beam propagating in a plasma with an index of refraction given by

$$n = n_0 + n_2 E_0^2, \tag{A1}$$

where n_0 is the linear refraction index, and $\delta n = n_2 E_0^2$, a nonlinear increment proportional to E_0^2, that is, the laser intensity. Such a term may arise as a consequence of the χ_3 term in the medium polarization and is the cause of self-focusing and filamentation. While in normal fluids the term n_2 may be positive or negative, in plasmas n_2 is always greater than 0. Since for a laser beam the intensity is always peaked on axis, we have a refraction index maximum on axis, and, since $v = c/n$, the external part of the beam will travel at higher velocity and the beam will focus. This is the whole-beam self-focusing case. In reality, it is more common for the self-focusing process to take place on smaller scales and for the beam to break in smaller parts which will focus independently originating laser "filaments" in the plasma.

It is possible to evaluate the growth of plasma filaments with radius r_f with the formula[17]

$$\alpha_{FI} = [\alpha_{PM} k_\perp^2/k_0^2 + \alpha_{TM} - (k_\perp^2/2k_0)^2]^{1/2}, \tag{A2}$$

where α_{FI} is the spatial growth rate, k_0 is the laser radiation wave number, and $k_\perp = 2\pi/\lambda_\perp$ with $\lambda_\perp = 4r_f$ the "wavelength" associated with the filament. The two terms α_{PM} and α_{TM} give the contribution due to thermal and ponderomotive effects which can both contribute to self-focusing by expelling electrons from the region where intensity is higher and hence increasing the local index of refraction. On the contrary, the term $k_\perp^2/2k_0$ represents the negative contribution of diffraction. For instance, if we consider the length of growth of the filamentation instability $1/\alpha_{FI}$ as a function of $\lambda_\perp$ for a neodymium laser and a homogeneous plasma with density $n_e = n_c/100$, $Z = 2$, and $T_e = 50$ eV and $I \simeq 10^{13}$, that is, the conditions of our experiment in helium gas, we see that $1/\alpha_{FI}$ increases dramatically for $\lambda_\perp \leq 5 \times 10^{-3}$ cm, and hence filamentation is impossible in these conditions. On the other hand, $1/\alpha_{FI}$ is practically constant for $\lambda_\perp > 5 \times 10^{-3}$ cm and is $\simeq 2 \times 10^{-2}$ cm. This means that it is possible to have self-focusing when $r_f > 12.5$ μm, if the plasma is longer than 2×10^{-2} cm.

The above results have been obtained using the classical formulas for α_{TM} and α_{PM} derived in the framework of the Spitzer–Harm theory of heat transport. In the case of nonlocal electron heat transport, a more complete theory has been formulated by Epperlein.[18]

We must note, however, that this linear theory of self-focusing is only good to evaluate the beginning of the instability. While the instability develops, the local laser intensity may change drastically and the conditions for the growth of filaments with smaller r_f may be reached. An indication of the final stages of the FI may be given by evaluating the minimum allowable filament radius in a plasma of given conditions. This may be calculated by assuming saturated (i.e., "empty") filaments and by writing the conditions for total internal reflection of the laser radiation inside the filament. For $n_e \ll n_c$ this gives

$$r_{min} = \frac{0.3c}{e}\left[\frac{\pi m_e}{n_e}\right]^{1/2}. \tag{A3}$$

This minimum size radius is reached over a "focusing" length, which, when considering only ponderomotive effects (which may be dominant for smaller filaments), is given by

$$l_{SF} = \frac{\omega_L}{\omega_p}\frac{v_e}{v_{os}}a, \tag{A4}$$

where v_e is the electron thermal velocity, $v_{os} = eE/\omega_L m_e$ is the quiver velocity of electrons in the wave electric fields, and a is the initial beam radius.

We see that l_{SF} decreases with $\omega_p v_{os}$, that is, the conditions for optimal growth of the filament instability are reached at smaller plasma densities for higher laser powers, or lower powers for higher densities.

The presence of filaments in the conditions of our experiment in helium gas were independently studied in an experiment at IFAM.[17] By using double-pulse holographic interferometry and by

studying the redistribution of ω light coming out of the plasma, it was possible to show that the laser beam was undergoing whole beam self-focusing while filaments were developing inside the beam. In particular, up to 40% of laser light was diffused at large angles (up to 14°). This could be produced by light diffracted on filaments of radius $\simeq 2.7$ μm. We note that for $n_e \simeq n_c/100$ (i.e., 150 Torr gas pressure at which the effect was more pronounced) from (A3) we get $r_{min} = 3$ μm.

Received 19 March 1993.

Résumé

Le mécanisme de génération de seconde harmonique dans les plasmas sous-critiques est examiné. Il est montré que la filamentation et l'auto-convergence du faisceau laser dans le plasma peuvent détruire la symétrie de densité du plasma et générer la seconde harmonique due aux électrons libres. Du même coup, l'émission de la seconde harmonique peut être utilisée pour étudier les paramètres du plasma et diagnostiquer le mécanisme de filamentation du faisceau laser lui-même.

References

1. N. Bloembergen, R.K. Chang, S.S. Jha, and C.H. Lee Phys. Rev. Lett. **174**, 813 (1968).
2. Y.R. Shen, *The Principles of Nonlinear Optics* (J. Wiley & Sons, NY, 1975), p. 8.
3. L.L. Landau and E.M. Lifshitz, *Teorija Polja* (MIR ed., Moscow, 1976).
4. J.D. Jackson, *Classical Electrodynamics* (J. Wiley & Sons, NY, 1975).
5. K. Miyazaki, T. Sato, and H. Kashiwagi, Phys. Rev. Lett. **43**, 1154 (1979).
6. T. Mossberg, A. Flushberg, and S.R. Hartman, Opt. Commun. **25**, 121 (1978).
7. D.S. Bethune, Phys. Rev. A **23**, 3193 (1981).
8. I. Deha, D. Batani, G.P. Banfi, F. Bianconi, A. Giulietti, D. Giulietti, L. Nocera, and E. Schifano, in *Inertial Confinement Fusion*, edited by A. Caruso and E. Sindoni (Ed. Compositori, Bologna, 1988), p. 359.
9. D. Batani, F. Bianconi, A. Giulietti, D. Giulietti, and L. Nocera, Opt. Commun. **70**, 38 (1989).
10. A. Yariv, *Quantum Electronics* (J. Wiley & Sons, NY, 1975).
11. L.A. Gizzi, D. Batani, V. Biancalana, M. Borghesi, P. Chessa, I. Deha, A. Giulietti, D. Giulietti, E. Schifano, and O. Willy, in *Laser Interaction and Related Plasma Phenomena*, edited by G.H. Miley and H. Hora (Plenum, NY, 1992), Vol. 10.
12. R.A. London and M.D. Rosen, Phys. Fluids **29**, 11 (1986).
13. J.A. Stamper, R.H. Lehmberg, A. Schmitt, M.J. Herbst, F.C. Young, J.H. Gardner, and S.P. Obenschain, Phys. Fluids **28**, 2563 (1985).
14. A. Giulietti, D. Giulietti, D. Batani, V. Biancalana, L. Gizzi, L. Nocera, and E. Schifano, Phys. Rev. Lett. **63**, 524 (1989).
15. E. Schifano, S. Baton, C. Labaune, T. Jalinaud, V. Biancalana, and D. Giulietti, *Rapport Scientifique 1991*, (LULI, Ecole Polytechnique, Palaiseau, 1991), p. 47.
16. P. E. Young, H. A. Baldis, T.W. Johnson, W.L. Kruer, and K.G. Estabrook, Phys. Rev. Lett **63**, 2812 (1989).
17. D. Giulietti, A. Giulietti, M. Lucchesi, and M. Vaselli, J. Appl. Phys. **58**, 2916 (1985).
18. E.M. Epperlein, Phys. Rev. Lett. **65**, 2145 (1990).

D. Batani
Dipartimento di Fisica, Università degli Studi
20133 Milano, Italy

A. Giulietti, V. Biancalana, F. Bianconi, M. Borghesi, P. Chessa, D. Giulietti, L. Gizzi
Istituto di Fisica Atomica e Molecolare, CNR
56100 Pisa, Italy

I. Deha
Université H. Boumedienne
Algers, Algery

E. Schifano
LULI, École Polytechnique
Palaiseau, France